A Portable MIMO Testbed and Select Channel Measurements

Paul Goud Jr., Robert Hang, Dmitri Truhachev and Christian Schlegel
Department of Electrical and Computer Engineering,
University of Alberta, Edmonton, Canada

November 29, 2004

Abstract

A portable 4x4 multiple-input multiple-output (MIMO) testbed that is based on field programmable gate arrays (FPGAs) and which operates in the 902 - 928 MHz ISM band has been developed by the High Capacity Digital Communications (HCDC) laboratory at the University of Alberta. We present a description of the HCDC testbed along with MIMO channel capacities that were derived from measurements taken with the HCDC testbed for three special locations: a narrow corridor, an open field that is surrounded by a metal fence and a parkade. The locations are special because the channel capacities are different from what is expected for a typical indoor or outdoor channel. Where possible a ray tracing analysis has been performed to explain the discrepancies. The discrepancies between the measured and expected channel capacities demonstrate the value of a MIMO testbed in optimizing the throughput for a location.

Keywords: MIMO, testbed, wireless, measurements, capacity

1 Introduction

Multiple-input, multiple-output (MIMO) wireless technology, with its promise to increased channel capacities, is now being considered for use in commercial systems. For example, there have been many proposals to include MIMO technology in the upcoming 802.11n standard for wireless local area networks (WiLAN) [1]. The IEEE 802.11n Task Group was created to make specifications for WiLAN systems (e.g. home video networks, voice-over-IP) that achieve a much higher transmission rate than what is currently possible with the 802.11a/g standards. The goal for the next generation WiLAN standard is a data throughput between 100 and 200 Mbits/sec. While the generic term MIMO generically means multiple-input multiple-output, however, in this paper we use it synonymously for a wireless with multiple inputs/outputs, i.e., a multiple antenna channel.

The successful deployment of commercial MIMO systems will require a solid understanding of the channel conditions. There have been many wireless channel models developed that emulate propagation conditions and can be used to provide estimates of MIMO channel capacity. For example, a simple model that is frequently used in simulation studies of Rayleigh fading conditions uses independent identically distributed (i.i.d.) Gaussian random generators to derive the values for each element of a MIMO channel gain matrix [2] [3]. More sophisticated wireless channel models attempt to account for multiple scatterers and their locations [4] [5]. Despite their complexity, even these more sophisticated models make many assumptions and ignore common propagation effects such as refraction, diffraction and reflection loss, or correlations among the different antenna elements. The many assumptions inherent in these models can result in MIMO channel capacity estimates for a location that have large error. The most accurate method to determine the capacity of a MIMO system at a given site is through an analysis of channel measurements.

The collection of the measurements mandates the use of a testbed that can accurately measure the relative gains and phases for all the elements in a MIMO channel gain matrix. In this article, we profile several locations

where the MIMO channel capacities we measured with our testbed are different from what would be expected for general indoor or outdoor channels. In order to explain the discrepancies, we analyze the location and in some cases perform a detailed ray tracing analysis.
In Section 2, we describe several MIMO testbeds that have been developed by different research teams. Section 3 is a review of the basics MIMO channel communications. Our own MIMO testbed design is presented in the fourth section. Channel measurements for some interesting locations are given in Section 5 and thoroughly examined. Finally, Section 6 provides a conclusion.

2 Background

In addition to the MIMO testbed that has been developed at the University of Alberta and is described later in this paper, several other research teams have developed similar testbeds. We will briefly describe the design and unique features of some of them.
A research team at Brigham Young University has developed a 4 MIMO prototyping testbed that operates at 2.45 GHz [6]. Both the transmitter and receiver stations are based on fixed point digital signal processing (DSP) microprocessor development boards and use custom four channel radio frequency (RF) modules. At each station, one DSP processor performs filtering and other operations for the signal to or from one antenna. A computer at the transmitter station generates the data streams and final processing is performed by a computer at the receiver station. System synchronization signal is obtained through a 10 MHz reference signal that passes from the transmitter to the receiver station.
Another MIMO testbed has been developed at Rice University in Houston, Texas [7] and operates at 2.4 GHz. This testbed is similar to our testbed in that its hardware is based on a field progammable gate array (FPGA) development board. Each FPGA board has two digital to analog converters (DACs) and two analog to digital converters (ADCs). Off-the-shelf RF up/downconverter boards from National Instruments are also used. A novel feature of the Rice University testbed is its ability to incorporate commercial RF channel emulators. Each emulator can model fading channels such as Rayleigh, Ricean and Nakagami.
A final testbed of interest is the Turbo MIMO-OFDM system that was built at the University of Bristol [8]. This system operates at 5 GHz and uses a DSP microprocessor development board for the baseband processing. What makes the Bristol system unique is their scheme for timing recovery and obtaining channel state information at the receiver. These processes are accomplished through the use of preambles that start every frame of data. Each transmitter has a preamble that is orthogonal to all others and has an exclusive timing slot. At the receiver, the signal from each receiver antenna is processed by an autocorrelation routine. This routine determines the peak autocorrelation timing for each preamble and uses the information it obtains to calculate the channel state information.

3 The Multi-Antenna MIMO Channel

3.1 Channel Model and Capacity

A MIMO transmission system uses N_t transmit and N_r receive antennas. Each antenna i transmits discrete symbols from a complex symbol alphabet each with energy E_{si} per signaling interval, such that $\sum_i E_{si} = E_s$ is constant for each use of the channel. These transmit symbols are modulated by a suitable pulse waveform, up-converted to the desired transmission band, and sent over the N_t transmit antennas. The signals from the receive antennas are mixed down to baseband, sampled, and fed into the receiver.
The wireless transmission channel is a linear channel to a high-degree of accuracy, and, provided that timing recovery can be accomplished, the received sampled complex signal y_{jl} consisting of an in-phase and a quadrature component for the j^{th} receive antenna at time l is given by

$$y_{jl} = \sum_{i=1}^{N_t} \sqrt{E_{si}} h_{ij} c_{il} + \eta_{jl} \tag{1}$$

where η_{jl} is a sample of circularly symmetrical complex Gaussian noise with variance N_0, c_{il} is the sampled transmitted signal and h_{ij} is the normalized complex *path gain* from transmit antenna j to receive antenna i. It

contains all linear effects on the signal, such as propagation power loss and phase shifts, fading due to multipath, cross-talk, antenna coupling, and polarization. This model furthermore assumes that the symbol rate is low enough such that frequency selectivity caused by time-of-arrival differences between various multipath replicas of the received signal is not an issue that manifests itself noticeably. This implies symbol rates of about 1 Mbaud or less for indoor transmission, and about 50 kbaud or less for outdoor situations [9].
The entire MIMO channel can now succinctly be characterized by the linear algebraic relationship

$$\boldsymbol{y} = \boldsymbol{H}\boldsymbol{A}\boldsymbol{c} + \boldsymbol{n}; \qquad \boldsymbol{A} = \begin{bmatrix} \sqrt{E_{s1}} & & & \\ & \sqrt{E_{s2}} & & \\ & & \ddots & \\ & & & \sqrt{E_{sN_t}} \end{bmatrix} \tag{2}$$

$\boldsymbol{H}$ is an $N_t \times N_r$ rectangular matrix of channel gains h_{ij} and $\boldsymbol{c}$ is a vector of N_t transmitted symbols c_{il}.
The information theoretic capacity of the discrete channel in (2) can be calculated from basic information theoretic concepts [10] as

$$C_I = \log_2 \det\left(\boldsymbol{I} + \frac{\rho}{N_t}\boldsymbol{H}\boldsymbol{E}\boldsymbol{H}^{+}\right) \qquad \text{[bits/channel use]}, \tag{3}$$

where $\rho = \frac{E_s}{N_0}$ is the signal-to-noise ratio per symbol,

$$\boldsymbol{E} = \frac{1}{E_s}\begin{bmatrix} E_{s1} & & & \\ & E_{s2} & & \\ & & \ddots & \\ & & & E_{sN_t} \end{bmatrix} \tag{4}$$

and $\boldsymbol{H}^{+}$ is the conjugate transpose of $\boldsymbol{H}$. Since the channel parameters are time-varying, C_I is interpreted as the "instantaneous" channel capacity for a given channel realization $\boldsymbol{H}$. For a time-varying channel this capacity has to be averaged over all realizations of the MIMO channel matrix $\boldsymbol{H}$ to calculate the ergodic channel capacity $C = E_{\boldsymbol{H}}(C_I)$. Telatar [11] has presented closed form solutions for C in the case where the h_{ij} are independent complex Gaussian fading channel gains.
The matrix $\boldsymbol{H}$ can be decomposed using the singular value decomposition (SVD) [12] $\boldsymbol{H} = \boldsymbol{U}\boldsymbol{D}\boldsymbol{V}^{+}$ where $\boldsymbol{U}$ and $\boldsymbol{V}$ are *unitary matrices*, and the matrix $\boldsymbol{D}$ contains the singular values $\{d_n\}$ of $\boldsymbol{H}$ on its diagonal, which are the positive square roots of the non-zero eigenvalues of $\boldsymbol{H}\boldsymbol{H}^{+}$ or $\boldsymbol{H}^{+}\boldsymbol{H}$. This allows the instantaneous capacity to be written in terms of the singular values as

$$C_I = \sum_{n=1}^{N} \log_2\left(1 + \frac{d_n^2 E_n}{N_0}\right) \rightarrow C_W = \sum_{n=1}^{N} \log_2\left(\frac{d_n^2 \mu}{N_0}\right) \tag{5}$$

and the maximizing energy levels for each subchannel are found via the the well-known waterfilling theorem [13] as

$$E_n = \mu - \frac{N_0}{d_n^2}; \qquad N_0/d_n^2 < \mu \tag{6}$$

$$E_n = 0; \qquad N_0/d_n^2 \geq \mu \tag{7}$$

leading to the waterfilling capacity C_W in (5).
However, if channel knowledge is not available at the transmitter the only choice is to distribute the energy uniformly over all component channels, using $E_n = E_s./N_t$. This special case is know as the *Symmetric Capacity*. Fundamentally, the capacity of a MIMO channel is governed by the singular values of $\boldsymbol{H}$ which determine the channel gains of the independent equivalent parallel channels resulting from the SVD.

3.2 MIMO Channels: Potential and Limitations

If the channel paths h_{ij} are uncorrelated, as happens when there is a multitude of scatterers that reflect the radio waves between transmitters and receiver, a typical observed channel realization will be of high rank with

eigenvalues of $\boldsymbol{H}\boldsymbol{H}^{+}$ distributed according to a Wishart distribution [11]. In this case the MIMO capacity will grow nearly linearly with the number of inputs and outputs, i.e., if we let $N = \min(N_r, N_t)$, then $C_I = O(N)$. If, however, the component channels show strong correlation, such as occurs in scatter-free long-distance wireless connections, e.g. in a satellite-ground radio link, or approximately in the green field and narrow corridor measurements discussed below, the rows $\boldsymbol{h}_j$ of $\boldsymbol{H}$, the *array response vectors*, become approximately equal, and $\boldsymbol{H}$ has only one non-zero singular value, $d^2 = N_t N_r$. As a result

$$C_{\text{low}} \approx \log_2 (1 + \rho N_r) \tag{8}$$

In this case the channel capacity grows only logarithmically with the number of (receive) antennas, and the system realizes only the power gain provide by having a larger virtual receive antenna, and not the diversity gain realized by a high-rank channel.
Real-world situation will lie somewhere between these two extremes, with the capacity determined by the complex propagation environment in which the system has to function. This leads to the necessity to carefully analyze and measure such candidate environments to obtain precise values.
Furthermore, the capacity potential of a MIMO channel requires relatively a high channel signal-to-noise ratio E_s/N_0, for otherwise $\log(1 + x) \approx x$ for small x, and

$$C_{\text{low}} \approx N_r \rho \tag{9}$$

also grows linearly with N, and no diversity gain can be realized, irrespective of whether the channel has high rank or not. Communications is fundamentally power limited and the additional dimensionality offered by a "high-rank" MIMO channel cannot be exploited.

3.3 MIMO Processing versus Beam Steering

In real world propagation scenarios, signal correlation is an important effect, and if the effective rank of a MIMO channel is reduced by strong correlation, that is, many of the SVDs of $\boldsymbol{H}$ will collapse, limiting the capacity of the channel, as can be seen from equation (5). If the channel rank is low, beam-steering is an appropriate choice, since no significant capacity is being lost. Beam steering in its simplest form can be accomplished via channel inversion either at the receiver, or at the transmitter, as illustrated in left-hand diagram in Figure 1. More specifically, the channel of equation (2) is modified by an inversion filter to

$$\boldsymbol{y}_{\text{beam}} = \boldsymbol{H}^{-1}\boldsymbol{y} = \boldsymbol{H}^{-1}(\boldsymbol{H}\boldsymbol{A}\boldsymbol{c} + \boldsymbol{n}) = \boldsymbol{A}\boldsymbol{c} + \boldsymbol{n}' \tag{10}$$

For a 4×4 MIMO channel beam-steering via channel inversion creates 4 parallel interference-free sub-channels which can be processed independently. However, on a full-rank MIMO channel, this channel inversion causes significant noise enhancement, or energy loss. Alexander et. al. [14] have calculated this loss in the context of a code-divsion multiple-access (CDMA) framework for i.i.d. component channels, which for a 4×4 MIMO system amounts to 6dB. An option to alleviate this loss is to suppress only 2, rather than 3 of the interfering channels, shown on the right-hand side of Figure 1, by a partial inversion filter which generates

$$\boldsymbol{y}_{\text{beam}} = \boldsymbol{P}\boldsymbol{y} = \boldsymbol{P}(\boldsymbol{H}\boldsymbol{A}\boldsymbol{c} + \boldsymbol{n}) = \begin{bmatrix} h_{11} & h_{12} & & \\ h_{21} & h_{11} & & \\ & & h_{33} & h_{34} \\ & & h_{43} & h_{44} \end{bmatrix} \boldsymbol{c} + \boldsymbol{n}' \tag{11}$$

two 2×2 sub-channels. The analysis via projection operations presented in [14] is applicable, and it can be shown that this process suffers an energy loss of 3dB if the component channels are i.i.d. distributed.
This situation generalizes to correlated channels with reduced effective rank, in the sense that little loss in capacity is suffered if the low-rank channels are switched off (see for example [15] and references therein). In other words, if a 4×4 channel with significant correlation has only two significant eigenvalues, two of the transmitters can be switched off, creating a 2×4 channel with of virtually the same capacity. Since we now have "extra" receive antennas, we can invert the channel with the (pseudo) inverse of the 2×4 channel matrix $\boldsymbol{H}$ and obtain two channels, each loosing only 3dB in signal-to-noise ratio w.r.t. an interference-free channel. Additionally, if the channel knowledge is available at the transmitter, pairs of antennas would be combined to

achieve antenna gain for both of these channels. Achievable capacities and losses in terms of signal-to-noise ratio or spectral efficiency can quite easily be computed for each situation.
If, on the other hand, full inversion of all channels according to (10) is attempted on a reduced-rank channel, the noise enhancement (energy loss) is worsened since the filter is attempting to compensate for the very small SVDs, rendering this method useless. In general, the rank of the channel determines how many independent transmissions channels can be supported and need to be created in order to exploit the capacity of the MIMO channel. Additional dimensions, in the form of redundant antennas, are then used to help steer the antenna patterns, achieving transmission gain.
In this light, optimal transmission via pre-filtering and post-filtering by the matrices resulting from the SVD decomposition can be viewed as transmitter-receiver matched beam-steering.

4 Testbed Description

The iCORE HCDC Lab has developed a flexible 4×4 MIMO measurement setup that allows real-time characterization of MIMO wireless channels in a flat-fading environment. The measurement setup determines the coefficients of the 4×4 MIMO transmission matrix.
The MIMO measurement setup consists of a transmitter and receiver that operate in the 902-928MHz ISM band. The transmitter, shown in Figure 2, is made up (from right to left) of a baseband board connected to an upconverter radio-frequency (RF) board that is wired to four antennas. The baseband board generates four orthogonal m-sequence overlaid Walsh codes for each of the four antennas using FPGAs. A spreading gain of 32 allows accurate estimation of the coefficients of the MIMO channel matrix. The codes are modulated using binary phase shift keying (BPSK) and are upconverted to the 900MHz ISM band by the RF board.
The receiver is made up of four antennas wired to a downconverter RF board which is connected to a baseband board similar to that of the transmitter. The downconverter RF board simply shifts the signals received on the antennas to an intermediate frequency (IF) that can be sampled by the baseband board. This IF signal is downconverted internally in the FPGA for further baseband processing. The FPGA recovers the chip timing using a novel synchronization algorithm than can operate in low signal-to-noise ratio environments [16]. Once synchronization is achieved, the correlations of all possible paths of the 4×4 MIMO channel are computed to obtain the coefficients of the channel matrix, $\boldsymbol{H}$, of the MIMO channel at a rate of 15625 matrices per second. A computer is used for the real-time display the MIMO channel matrices and statistics.
The benefit of a real-time MIMO testbed is manifold. It allows real-world characterization of MIMO propagations that are difficult to model. It allows researcher to quickly find channels with interesting characteristics (e.g. outdoor channels with high matrix rank or indoor channel with low matrix rank) in order to study them and gain a better understanding of the advantages and limitations of MIMO communications. Finally, these MIMO channel matrices can be stored and used in link level simulations of communications systems in order to obtain results that are typical of real-world situations.

5 Channel Measurements for Select Channels

The purpose of a MIMO testbed is to study channel situations which are not readily accessible to an analytical treatment, or where the propagation environment makes analytical predictions inaccurate or infeasible. In this section we present a select number of unusual channel situations with their MIMO measurements. In some cases, we offer simple analytical models which capture the essence of the MIMO channel as it pertains to its information theoretic capacity. Many of the measurements are available to other research teams to download from our MIMO website (www.ece.ualberta.ca/ mimo). In particular, we will present three locations we found to be of interest: a narrow corridor, an open field with a nearby chain fence and a parkade [17]. A signal to noise ratio (SNR) of 20 dB was used for all our channel capacity calcuations.

5.1 Narrow corridor

A narrow corridor is an intriguing location for making MIMO channel measurements because of its tendency to act like a thin pipe and increase the correlation between the signals at the receiver antennas. A previous corridor study [18] of MIMO channel capacity at 1.95 GHz found that channel capacity decreased with distance down

the hall. The authors believe this decrease is due to the keyhole effect. This behaviour is different from the rich multipath environment that is typical of indoor offices even though corridors are commonly found in office settings.

Our investigation of MIMO channel capacity in a narrow corridor occurred in the northern corridor on the 5th floor of the Civil/Electrical Engineering Building at the University of Alberta campus. The corridor has the dimensions of 4m wide by 3m in height and has walls constructed of concrete blocks and a suspended ceiling. The map in Figure 3 shows the transmitter and receiver locations. The transmitter was placed at one end of the hall and the receiver station was put at three different locations. An analysis of our measurement campaign data confirms the findings of the previous study. Table 1 shows that the channel capacity drops as the receiver cart is moved down the hall.

Figure 7 gives an intuitive understanding of what occurs. Radio waves (ray A) that strike the concrete walls at a small angle of incidence θ will require many reflections to reach the receiver. Since power is lost with each reflection, multi-reflected rays will be heavily attenuated at the end of the hall. Those waves that strike a wall with a glancing blow (ray C) will require fewer reflections to reach the receiver and thus suffer less attenuation. In addition to this, studies [19] of the RF reflection properties of concrete blocks have shown that smaller angles of incidence have lower power reflection coefficients. Therefore, multi-bounce rays are additionally attenuated by having a lower reflection coefficient with every reflection. These effects explain why propagation along a narrow corridor should be very effective in eliminating multipath components and reducing the MIMO channel rank.

The greatly diminished multipath propagation environment makes it easy to perform a ray-tracing analysis of the site. The reflection coefficient for a radio signal off a plane surface can calculated when five values are known: the wavelength, the relative dielectric constant of the material, the conductivity of the material, the polarization of the radio wave and the angle of incidence [20]. For concrete, a typical relative dielectric constant is 5 and a typical conductivity is 0.001.

A Matlab program was written which simulates the line-of-sight path, the radiation reflected off the floor, the once reflected rays off both of the walls and the twice reflected rays off the walls. Since our dipole antennas were vertically polarized, a vertically polarized reflection will occur off the floor and a horizontally polarized reflection will occur off the walls. A 180 degree phase shift will occur for a vertically polarized reflection with a large angle of incidence.

Reflection coefficients were calculated for all the rays for the three locations with our estimates of the incidence angles. These coefficients were used to calculate the complex signals at the receiver. Channel gain matrices were created by adding all the contributions and then the expected MIMO capacity was calculated. The average capacity values appear in the second column of Table 1. The actual channel capacities can be seen to closely match the predicted channel capacities.

5.2 Open field

A second measurement campaign that provided surprising results was the Corbett sports field location at the University of Alberta. Figure 4 is a map of the location. Since this location is an open field, it was our expectation that this would be close to an ideal nonscattering environment and our MIMO channel would have low rank. The closest buildings are many metres away and do not have a geometry that would easily lend themselves to reflecting rays back towards the receiver station.

A theoretical analysis of an open field environment [4] predicts that MIMO channel capacity will decrease as the distance between the transmitter and receiver stations increases. The further apart the two stations are, the closer the LOS path length are to being equal and, hence, the channel gain matrix should approach an all-ones matrix which has very low rank. In fact, a measurement campaign performed on a farm yielded exactly these results. The same station separations were used for both the farm and sports field locations. The average channel capacities for the farm are shown in the second column of Table 2.

Much to our surprise, the channel capacity on the sports field actually increased as the station separation increased. Our investigation into the unexpected results focused on a wire mesh fence with a height between 2m and 4m, which we had not noticed originally as a significant scatterer, located 25 m to the right of both the receiver and transmitter stations. It run in parallel to line-of-sight between the two stations. To the left of the stations there exists another fence that is curved and is at least 40m away.

As was done in the narrow corridor case, a ray tracing program was written for the location. The channel

simulation included the line-of-sight path, the radiation reflected off the ground and the reflected rays off the two fences. The vertically polarized reflection coefficient for the grassy ground was once again calculated with a typical relative dielectric constant of 10 and conductivity value of 0.005.
The different propagation distances were accounted for by including a free space attenuation factor with all the paths [21]. The capacity values from the program appear in the last column of Table 2. The simulated capacities increase with distance in a similar fashion to our measured values.

5.3 Parkade

There are several publications that describe MIMO measurement campaigns for indoor office environments and calculate the channel capacity [22] [23]. A parkade is different from an indoor office environment in several respects. First, a typical indoor office has building materials (e.g. gyproc, glass, wood) that are not found in a parkade. In addition, an indoor office environment usually has interior walls and doors that are not present in a parkade. We could find no previous published results for a parking lot location.
Level P1 of the underground parkade in the ECERF (Electrical and Computer Research Facility) building on the University of Alberta campus was selected for a MIMO measurement campaign. The ECERF parkade is a typical parkade in that it has concrete walls, floors and pillars. At the time the measurements were taken, many of the parking spots were filled with cars. The map in Figure 5 shows the location of the transmitter station and receiver measurement places.
The channel capacities calculated from our parkade measurements (see Table 3) were slightly lower than what we had measured for indoor office environments (typically about 20 bits/channel use for a 4×4 system). Thus, the features of an indoor office may be more effective in creating a rich multipath environment than the vehicles present in the parkade. The average channel capacities for locations L1, L2 and L3 are lower than those for locations L4 and L5. This is not surprising since a LOS path exists in the former cases.

6 Conclusion

In this paper, we have described our portable 4x4 MIMO testbed and presented the measured MIMO capacity for several special locations. The measured MIMO capacities for these locations are different from what would be calculated from general indoor and outdoor wireless propagation models. We have examined the special propagation effects that are occurring which in some cases has involved a ray-tracing analysis of the site. The channel capacities derived from the analysis are close to our measured values.
As mentioned earlier, MIMO technology is now being proposed for new wireless standards such as 802.11n WLAN systems. Because of the large variation in channel capacity that can occur, the implementation of future commercial MIMO wireless systems should be performed with a MIMO capacity measuring device similar to a MIMO testbed in order to optimize the throughput.

7 Acknowledgements

The authors gratefully acknowledge the funding for this work provided by the Alberta Informatics Circle of Research Excellence (iCORE), the Natural Sciences and Engineering Research Council (NSERC), the Canadian Foundation for Innovation (CFI) and the National Sciences Foundation (NSF) of the United States. Gratitude is also extended to Ivan Kocev and Tobias Kiefer of the University of Applied Sciences in Offenburg, Germany for their considerable effort in collecting MIMO channel measurements.

References

[1] P. Mannion, “IEEE pushes WLANs to ’nth’ degree,” *Electronic Engineering Times*, p. 8, July 5, 2004.

[2] D. Chizhik, F. Rashid-Farrokhi, J. Ling, A. Lozano, “Effect of antenna separation on the capacity of BLAST in correlated channels,” *IEEE Communications Letters*, vol. 4, no. 11, pp. 337-339, Nov. 2000.

[3] G.J. Foschini and M.J. Gans,“On limits of wireless communications in a fading environment when using multiple antennas,” *Wireless Personal Communications*, vol.6, no. 3, pp. 311-335, Mar. 1998.

[4] D. Gesbert, H. Bolcskei, D. Gore, A. Paulraj, "Outdoor MIMO wireless channels: models and performance prediction," *IEEE Transactions on Communications*, vol. 50, no. 12, pp. 1926-1934, Dec. 2002.

[5] D. Shiu, G. Foschini, M. Gans, J. Kahn, "Fading correlation and its effect on the capacity of multielement antenna systems," *IEEE Transactions on Communications*, vol. 48, no. 3, pp. 502-513, Mar. 2000.

[6] J. Wallace, B. Jeffs, M. Jensen, "A real-time multiple antenna testbed for MIMO algorithm development and assessment," *Proc. IEEE Antennas and Propagation Society Symposium, 2004*, pp. 1716 - 1719, June, 2004, Monterey, CA.

[7] P. Murphy, F. Lou, A. Sabharwal, J. Frantz, "An FPGA based rapid prototyping platform for MIMO systems," *Proc. Signals, Systems and Computers, 2003 The Thrity-Seventh Asilomar Conference on*, pp. 900 - 904, Nov. 2003, Pacific Grove, CA.

[8] T. Horseman, J. Webber, M. Abdul-Aziz, R. Piechocki, A. Nix, M. Beach and P. Fletcher "A testbed for evaluation of innovative turbo MIMO OFDM architectures," *Proc. Personal Mobile Communications Conference 2003 5th European* , pp. 453 - 457, 2003.

[9] *Guidelines for Evaluation of Radio Transmission Technologies for IMT-2000*, Recommendation ITU-R M.1225, 1997.

[10] T. Cover and J. Thomas, *Elements of Information Theory*. New York: Wiley, 1991.

[11] E. Telatar, "Capacity of multi-antenna Gaussian channels," *Eur. Trans. on Telecomm. (ETT)*, vol. 10, no. 6, Nov. 1999, pp. 585-596.

[12] R.A. Horn and J.C. Johnson, *Matrix Analysis*. New York: Cambridge University Press, 1990.

[13] R.G. Gallager, *Information Theory and Reliable Communication*. New York: Wiley, 1968.

[14] P.D. Alexander, L. Rasmussen, and C. Schlegel, A Class of Linear Receivers for Coded CDMA, *IEEE Trans. Commun.*, Vol. 45, No. 5, pp. 605-610, May 1997

[15] C. Schlegel, Z. Shi, M. Burnashev, "Asymptotically Optimal Power Allocation and Code Selection for Iterative Joint Detection of Coded Random CDMA", *IEEE Trans. Inform. Theory*, in revision.

[16] R. Hang, C. Schlegel, W. A. Krzymien, P. Goud Jr. "A Robust Timing Recovery Algorithm for Spread-Spectrum Packet Radio Systems," *Proc. 16th International Conference on Wireless Communications*, July 12-14, 2004, Calgary, AB, Canada.

[17] I. Kocev, T. Kiefer, *Implementation and capacity potential verification of multiple antenna transmission systems*, Master's thesis, University of Applied Sciences Offenburg, Sept. 2004.

[18] D. Porrat, P. Kyritsi, D. Cox, "MIMO capacity in hallways and adjacent rooms," *Proc. Global Telecommunications Conference, 2002 (GLOBECOM '02)*, pp. 1930 - 1934, Nov. 2002.

[19] W. Honcharenko, H. Bertoni, "Transmission and reflection characteristics at concrete block walls in the UHF bands proposed for future PCS," *IEEE Transactions on Antennas and Propagation*, vol. 42, no. 2, pp. 232-239, Feb. 1994.

[20] E. Jordan, K. Balmain, *Electromagnetic Waves and Radiating Systems*. Englewood Cliffs: second edition, Prentice-Hall Inc., 1968.

[21] M. Martone, *Multiantenna Digital Radio Transmission*. Norwood, MA: 1st edition, Artech House, 2002.

[22] A. Swindlehurst, G. German, J. Wallace, M. Jensen, "Experimental measurements of capacity for MIMO indoor wireless channels," in *Proc. Wireless 2003 Conference*, pp. 423-427, Calgary, Canada, July 2003.

[23] P. Goud Jr., C. Schlegel, R. Hang, W. Krzymien, Z. Bagley, S. Messerly, P. Watkins, V. Rajamani, "MIMO channel measurements for an indoor office environment," in *Proc. Wireless Communications, 2001. (SPAWC '01). 2001 IEEE Third Workshop on Signal Processing Advances in*, pp. 30-33, Taoyuan, Taiwan, Mar. 2001.

List of figures and tables

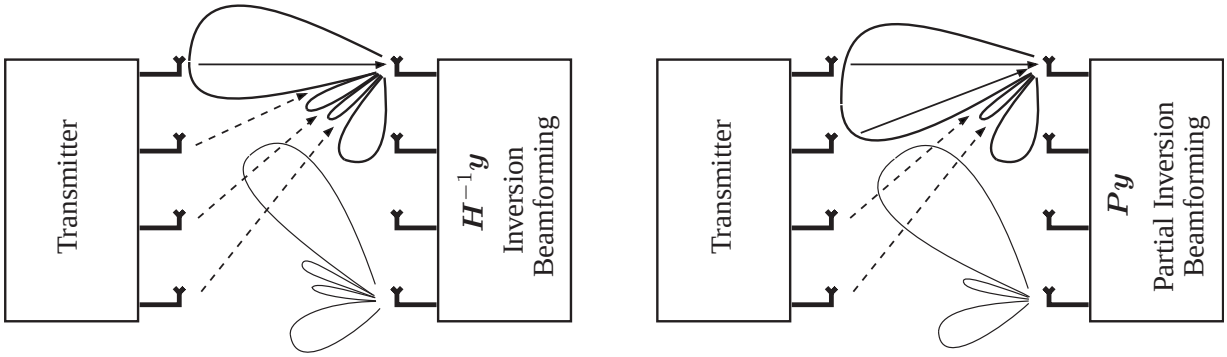

Figure 1: Illustration of beam-steering uses of multiple antenna systems.

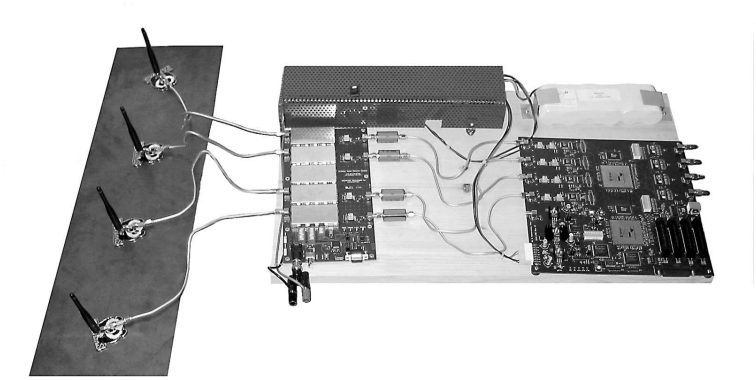

Figure 2: Photo of the MIMO Testbed

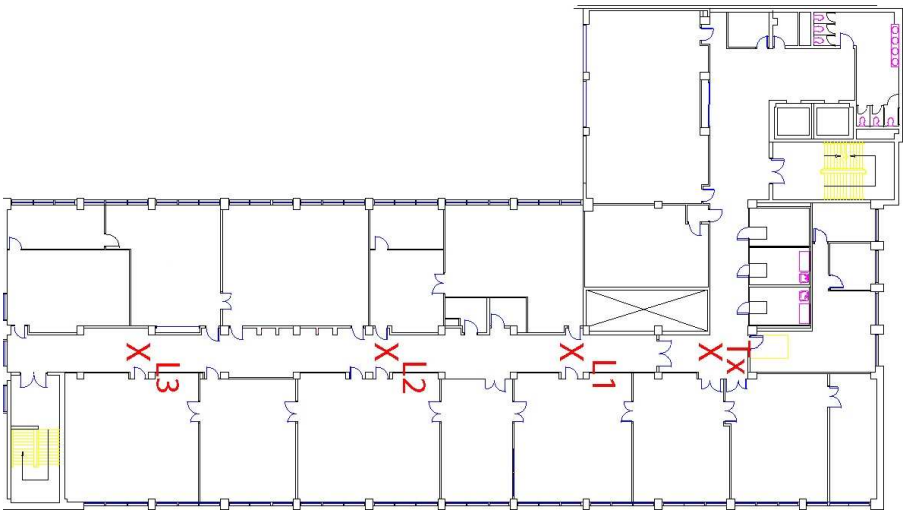

Figure 3: Corridor Map

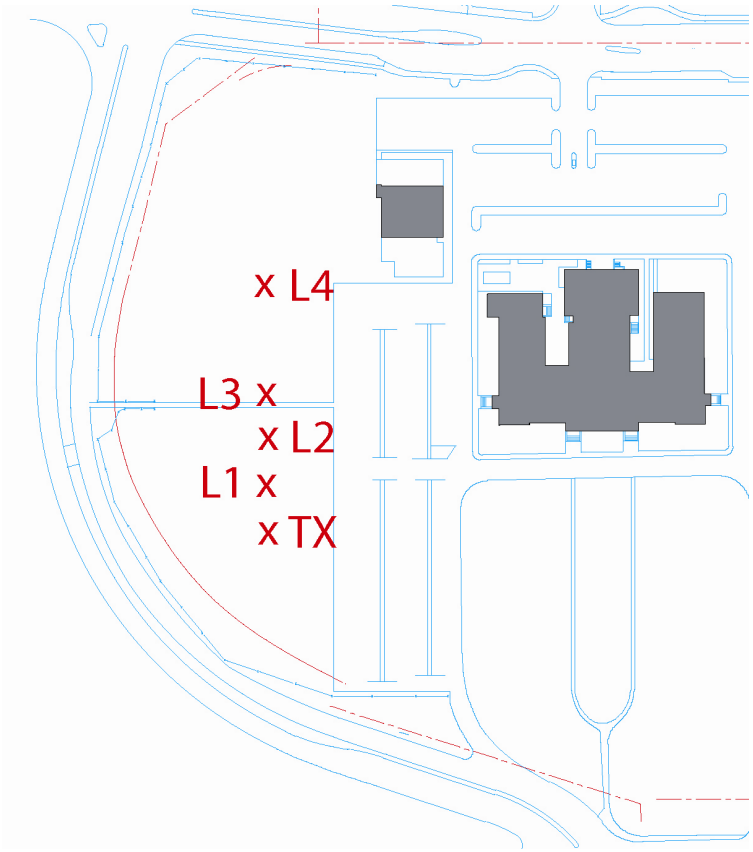

Figure 4: Coerbett Field Map

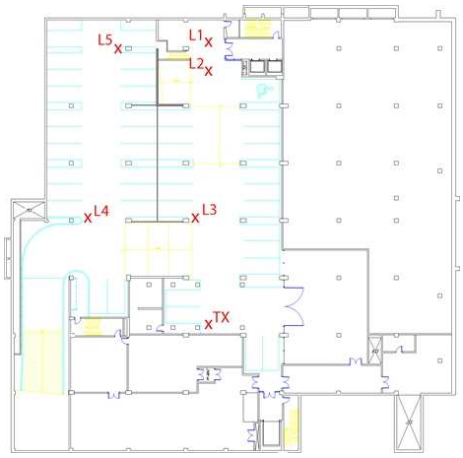

Figure 5: Parkade Map

Figure 6: Parkade Photo

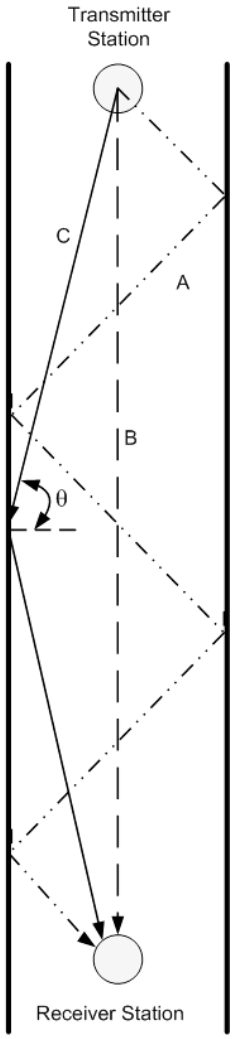

Figure 7: Corridor Diagram

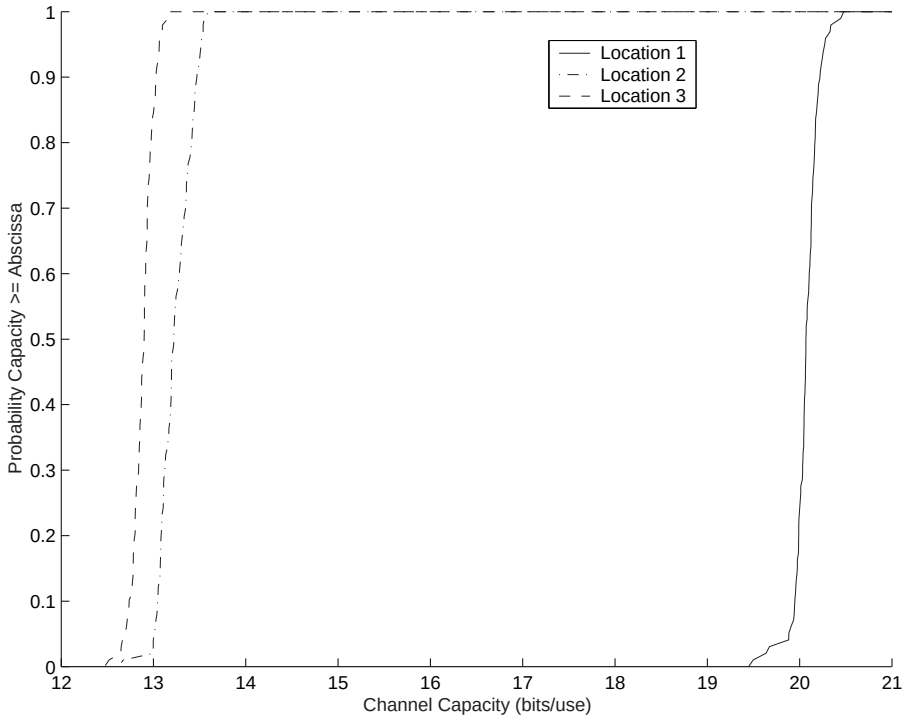

Figure 8: Capacity cdf

	Average Channel Capacity (bits/use)	Max. Channel Capacity (bits/use)	Min. Channel Capcity (bits/use)	Channel Capacity from the Model (bits/use)
Location 1	19.226	19.741	18.680	19.789
Location 2	12.270	12.553	12.062	14.244
Location 3	12.180	12.550	11.843	10.960

Table 1: Capacity in the Corridor

	UofA farm Measured Average Channel Capacity (bits/use)	Corbett Field Measured Average Channel Capacity (bits/use)	Fild with a fence Model Channel Capacity (bits/use)
Location 1 (20m)	11.314	11.097	13.526
Location 2 (40m)		17.097	15.668
Location 3 (60m)	9.383	18.079	16.646
Location 4 (100m)	9.860	19.439	15.980

Table 2: Capacity in the Field

	Average Channel Capacity (bits/use)	Max. Channel Capacity (bits/use)	Min. Channel Capcity (bits/use)
Location 1	15.972	16.865	15.287
Location 2	17.616	17.616	16.615
Location 3	14.231	16.616	13.008
Location 4	18.463	19.632	17.127
Location 5	18.752	19.994	17.717

Table 3: Capacity in the Parkade